




The effect of RNA polymerase V on 24-nt siRNA accumulation depends on DNA methylation contexts and histone modifications in rice

Kezhi Zheng^{a,1} , Lili Wang^{a,1}, Longjun Zeng^{b,1}, Dachao Xu^a , Zhongxin Guo^c, Xiquan Gao^a, and Dong-Lei Yang^{a,2} 

^aState Key Laboratory for Crop Genetics and Germplasm Enhancement, Nanjing Agricultural University, 210095 Nanjing, China; ^bAcademy for Advanced Interdisciplinary Studies, Nanjing Agricultural University, 210095 Nanjing, China; and ^cVector-borne Virus Research Center, Fujian Agriculture and Forestry University, 350002 Fujian, China

Edited by Craig S. Pikaard, Indiana University Bloomington, Bloomington, IN, and approved June 17, 2021 (received for review January 20, 2021)

RNA-directed DNA methylation (RdDM) functions in de novo methylation in CG, CHG, and CHH contexts. Here, we performed map-based cloning of *Osnrpe1*, which encodes the largest subunit of RNA polymerase V (Pol V), a key regulator of gene silencing and reproductive development in rice. We found that rice Pol V is required for CHH methylation on RdDM loci by transcribing long non-coding RNAs. Pol V influences the accumulation of 24-nucleotide small interfering RNAs (24-nt siRNAs) in a locus-specific manner. Biosynthesis of 24-nt siRNAs on loci with high CHH methylation levels and low CG and CHG methylation levels tends to depend on Pol V. In contrast, low methylation levels in the CHH context and high methylation levels in CG and CHG contexts predisposes 24-nt siRNA accumulation to be independent of Pol V. H3K9me1 and H3K9me2 tend to be enriched on Pol V-independent 24-nt siRNA loci, whereas various active histone modifications are enriched on Pol V-dependent 24-nt siRNA loci. DNA methylation is required for 24-nt siRNAs biosynthesis on Pol V-dependent loci but not on Pol V-independent loci. Our results reveal the function of rice Pol V for long noncoding RNA production, DNA methylation, 24-nt siRNA accumulation, and reproductive development.

RNA polymerase V | *Osnrpe1* | siRNA | rice

DNA methylation plays an essential role in silencing transposons and repetitive elements. RNA-directed DNA methylation (RdDM) is the main mechanism for de novo DNA methylation in plants (1–9). In the canonical RdDM pathway, a transcription factor-like protein SAWADEE HOMEODOMAIN HOMOLOG 1 (SHH1, also known as DNA-BINDING TRANSCRIPTION FACTOR 1, DTF1) and four chromatin remodeling proteins, CLSY1 to CLSY4, facilitate RNA polymerase IV (Pol IV) targeting and transcription (10–14). Pol IV transcribes targets into 25- to 50-nt small RNAs (P4-RNAs) (15–19), which are immediately transcribed into double-stranded RNAs (dsRNAs) by RNA-dependent RNA polymerase 2 (RDR2) (19, 20). The dsRNAs are cleaved by DICER-LIKE 3 (DCL3) to generate 24-nucleotide small interfering RNAs (24-nt siRNAs) (19, 21), which are loaded into ARGONAUTE 4 (AGO4) protein to form the silencing complex (22). Pol V recruits AGO4 via the AGO hook motif in the C-terminal domain (CTD). The siRNAs in AGO4 are believed to base pair with the nascent RNAs transcribed by Pol V (23, 24). In this process, DOMAINS REARRANGED METHYLTRANSFERASE 2 (DRM2) is recruited to the targets and catalyzes DNA methylation (25).

Pol V transcription and targeting depend on the DDR complex, which contains DEFECTIVE IN RNA-DIRECTED DNA METHYLATION 1 (DRD1), DEFECTIVE IN MERISTEM SILENCING 3 (DMS3), and RNA-DIRECTED DNA METHYLATION 1 (RDM1) (23, 24, 26). The recruitment of Pol V to targets requires the binding of SU(VAR)3-9 homologs SUVH2 and SUVH9 to methylated DNA (27, 28). Recent research has revealed that even on non-RdDM loci, Pol V transcription is dependent on the DDR complex, SUVH2, and SUVH9 (29). Pol V transcripts contain a

common uracil (U) at position 10, which is complementary to the 5' adenine (A) of the 24-nt siRNAs bound in the AGO4 protein (30), suggesting that AGO4 can slice Pol V transcripts. The slicing activity of AGO4 has been found to be essential for DNA methylation and siRNA production on a subset of RdDM targets (31, 32). These results indicate that the slicing of Pol V might be a key signal that initiates efficient de novo methylation.

In *Arabidopsis*, tomato, and *Brassica rapa*, the accumulation of nearly all 24-nt heterochromatic siRNAs is dependent on Pol IV, but accumulation of only a subset of siRNAs is dependent on Pol V (33–37). On the non-long terminal repeat (non-LTR) retrotransposons and helitrons, siRNA biosynthesis tends to depend on Pol V in *Arabidopsis* (34), suggesting that transposon identity might be a factor that determines whether siRNA production is dependent on Pol V. Based on the different roles of Pol IV and Pol V in siRNA production, researchers have hypothesized that Pol V could function as a component in a self-reinforcing loop in siRNA production and de novo DNA methylation (33, 34). According to this hypothesis, if the initial signal for recruitment of Pol IV-RDR2 is sufficiently strong, siRNA biosynthesis is independent of Pol V; if the initial signal is weak, however, the effect of Pol V on siRNA production will be pronounced (34). This hypothesis was supported by the finding that the accumulation of AGO4-dependent siRNAs on a subset of RdDM loci requires Pol

Significance

Rice RNA polymerase V (Pol V) influences the accumulation of 24-nucleotide small interfering RNAs (24-nt siRNAs) in a locus-specific manner. Accumulation of 24-nt siRNAs is dependent on Pol V on loci with high CHH methylation levels, low CG and CHG methylation levels, and high active histone modifications. In contrast, a low methylation level in the CHH context, high methylation levels in CG and CHG contexts, and enrichment of repressive histone modifications predispose 24-nt siRNA accumulation to be independent of Pol V. DNA methylation is essential for 24-nt siRNA biosynthesis on Pol V-dependent loci but not on Pol V-independent loci. Our results suggest that monocot Pol V-transcribed scaffold RNAs are essential for reproductive development and 24-nt siRNA biosynthesis on euchromatin.

Author contributions: D.-L.Y. designed research; K.Z. and L.Z. performed research; L.W. conducted bioinformatic analyses; D.X., Z.G., and X.G. contributed new reagents/analytic tools; D.-L.Y. analyzed data; and K.Z. and D.-L.Y. wrote the paper.

The authors declare no competing interest.

This article is a PNAS Direct Submission.

Published under the PNAS license.

¹K.Z., L.W., and L.Z. contributed equally to this work.

²To whom correspondence may be addressed. Email: dlyang@njau.edu.cn.

This article contains supporting information online at <https://www.pnas.org/lookup/suppl/doi:10.1073/pnas.2100709118/-DCSupplemental>.

Published July 21, 2021.

V, DRM2, and SHH1 (32). The locus-specific role of Pol V in siRNA production has been found in several plant species, but the underlying mechanism is not known.

Here, we used a genetic screen to identify and clone *OsNRPE1* as a key component in the silencing of transgene in rice. Mutation in *OsNRPE1*, which encodes the largest subunit of Pol V, greatly reduced seed setting, suggesting that Pol V as well as OsRDR2 and Pol IV play a vital role in the reproductive development of rice (38–40). Depletion of Pol V led to a substantial loss of CHH methylation on short transposons near genes. Moreover, siRNA accumulation was Pol V-dependent in a locus-specific manner. Analysis of DNA methylation contexts demonstrated that high CHH methylation combined with low CG and CHG methylation predisposes siRNA production to be dependent on Pol V, while siRNA production on loci with high CG and CHG methylation and with low CHH methylation tends to be independent of Pol V. In addition to observing the context bias for DNA methylation, we also observed the enrichment of H3K9me1 and H3K9me2 on loci that do not depend on Pol V for siRNA production and the enrichment of multiple active histone

modifications on loci that depend on Pol V for siRNA production. The transcriptional levels are much higher for genes adjacent to loci that depend on Pol V for siRNA production than for those adjacent to Pol V-independent loci. Our findings demonstrate that the degree to which siRNA production depends on Pol V in rice is probably determined by DNA methylation contexts and histone modifications. Rice has developed multiple epigenetic mechanisms to fine-tune gene expression in order to ensure proper development.

Results

Map-Based Cloning of Five Elements Mountain 3. *OsGA2ox1* encodes a gibberellin metabolism enzyme (41), and its ectopic expression in a japonica variety, TP309, resulted in transgenic plants (GAE) showing GA deficiency and dwarfism (38) (Fig. 1A and B and SI Appendix, Fig. S1A). Spontaneous silencing of the transgene 35S::*OsGA2ox1* in the transgenic plants resulted in plants (GAS) with normal plant height (38) (Fig. 1A and B and SI Appendix, Fig. S1A). Small-RNA sequencing (sRNA-seq) revealed that *OsGA2ox1* produced abundant 21- and 22-nt

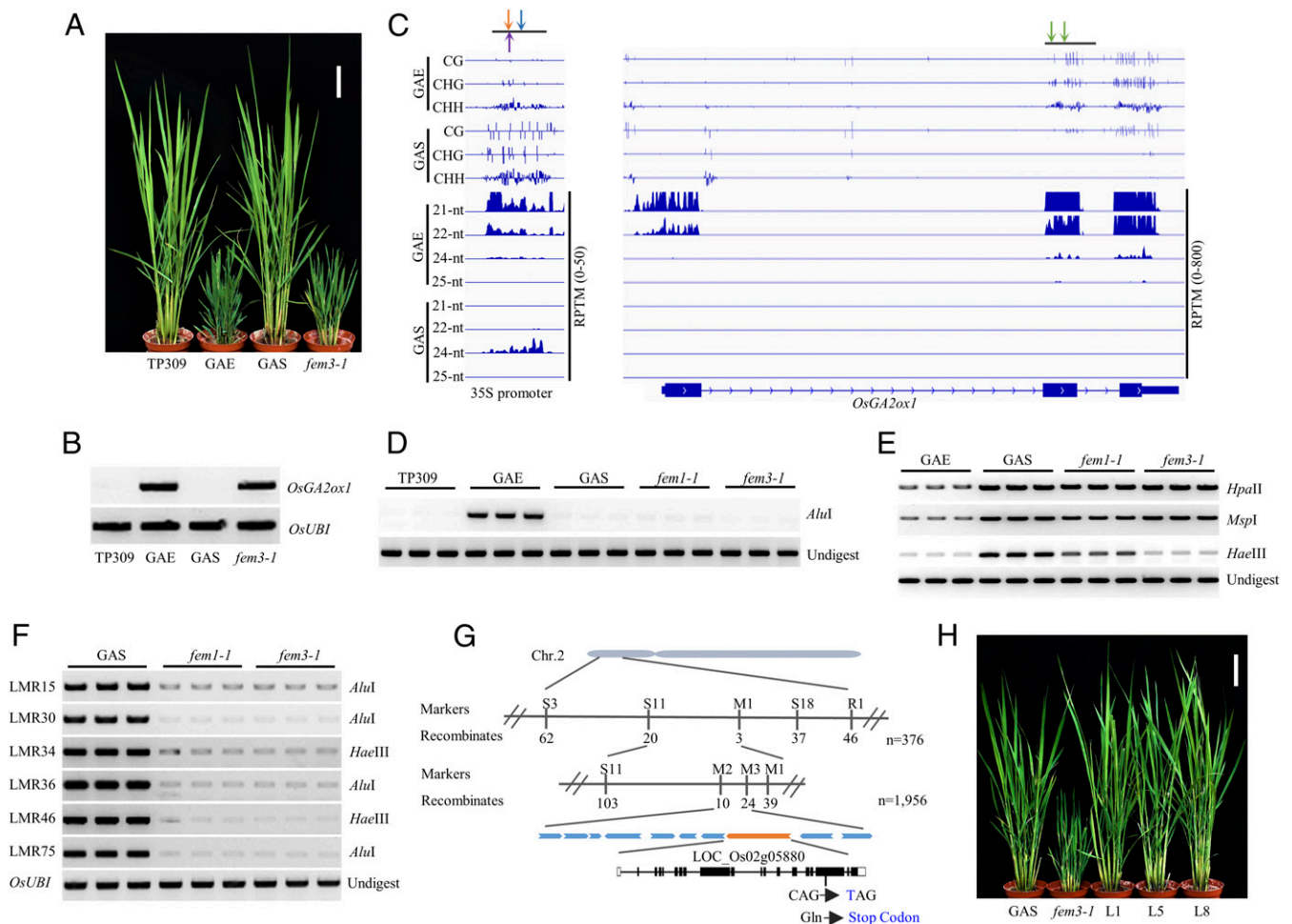


Fig. 1. Identification of the *fem3-1* mutant and map-based cloning of *FEM3*. (A) The morphologies of TP309, GAE, GAS, and *fem3-1* plants. (Scale bar, 10 cm.) (B) Transcript levels of *OsGA2ox1* as determined by semi-qRT-PCR in the indicated genotypes. *OsUbiquitin* (LOC_Os03g13170) served as the control. (C) Integrative genome browser image showing the methylation levels and siRNA abundance on the 35S promoter and *OsGA2ox1* in GAE and GAS. The arrows indicate cutting sites (orange for *MspI*; purple for *HpaII*; blue for *HaeIII*; and green for *AluI*). (D and E) DNA methylation levels on *OsGA2ox1* (D) and the 35S promoter (E) in GAE, GAS, *fem1-1*, and *fem3-1* as determined by Chop-PCR assay. Undigested DNA served as the control. (F) DNA methylation levels on six RddM loci in GAS, *fem1-1*, and *fem3-1* as determined by Chop-PCR assay. The template of the PCR was digested by *AluI* or *HaeIII*. *OsUbiquitin* (LOC_Os03g13170) served as the control with undigested DNA as template. (G) Diagram indicating the map-based cloning of *FEM3*. The recombinant number and molecular markers (Dataset S1) are indicated below and above the bars, respectively. The changes in DNA and protein sequences in *fem3-1* are indicated in blue. (H) Morphologies of the indicated genotypes. (Scale bar, 10 cm.)

siRNAs and relatively few 24-nt siRNAs on the exons of *OsGA2ox1* in GAE (Fig. 1C). Whole-genome bisulfite sequencing (WGBS) found that on 3' two exons of *OsGA2ox1*, there was methylation on CG, CHG, and CHH in GAE (Fig. 1C). In contrast, there was methylation on CG but not on CHG or CHH in TP309 (SI Appendix, Fig. S1B), suggesting that siRNAs are involved in establishing non-CG methylation on *OsGA2ox1* in GAE. Because the siRNAs on *OsGA2ox1* exons were eliminated, non-CG methylation disappeared in GAS (Fig. 1C). Chop-PCR assay confirmed that CHH methylation on *OsGA2ox1* is greater in GAE than in TP309 and is absent in GAS (Fig. 1D).

In GAE, the 35S promoter also produced abundant 21- and 22-nt siRNAs and relatively few 24-nt siRNAs (Fig. 1C); there were low DNA methylation levels in CG, CHG, and CHH on the 35S promoter in GAE (Fig. 1C). In GAS, the 21- and 22-nt siRNAs disappeared but 24-nt siRNAs increased. The DNA methylation levels on CG, CHG, and CHH increased substantially in GAS (Fig. 1C). Chop-PCR assay confirmed that DNA methylation in three contexts was higher in GAS than in GAE (Fig. 1E), suggesting that transcriptional gene silencing of 35S::*OsGA2ox1* probably occurs in GAS.

After using ethyl methyl sulfonate to treat GAS seeds, we isolated *five elements mountain 3* (*fem3*) rice plants with restored overexpression of 35S::*OsGA2ox1* (Fig. 1A and B and SI Appendix, Fig. S1A). In the *fem3* mutant, the CHH methylation level on the 35S promoter was lower than in GAS (Fig. 1E), while the levels of CG and CHG methylation in *fem3* were similar to

those in GAS, suggesting that *FEM3* probably regulates gene silencing by controlling CHH methylation on the 35S promoter. On the gene body of *OsGA2ox1*, the low methylation levels in the CHH context in GAS were also evident in the *fem3* mutant (Fig. 1D).

Beside the exogenous 35S promoter, six endogenous RddM loci (38) were examined for the effect of *FEM3* on CHH methylation. Chop-PCR assay showed that, like in *fem1*, CHH methylation in *fem3* was substantially lower than in GAS (Fig. 1F), demonstrating that *FEM3* controls CHH methylation on both transgene and endogenous genomic loci.

We performed map-based cloning of *FEM3* using 978 F2 plants with a GA-deficient phenotype that were generated from a cross between *fem3-1* heterozygous plants and Taichuang native 1 (TN1), an indica variety. The location of the candidate gene was narrowed to a region of ~68 kb on the short arm of chromosome 2, which contains 10 putative genes (Fig. 1G). Sequencing detected a single-base substitution (C-T) on the seventeenth exon of LOC_Os02g05880, which resulted in a premature stop codon and a truncated protein that lacked five repeats and a DEFECTIVE CHLOROPLASTS AND LEAVES (DeCL) domain (Fig. 1G and SI Appendix, Fig. S1C). To confirm that the point mutation in LOC_Os02g05880 was responsible for the *fem3-1* mutant phenotypes, we transformed its genomic DNA fragment with its 2-kb promoter into *fem3-1* plants for a complementary test. We obtained 18 independent transgenic lines including 15 positive and 3 negative lines. All positive line plants displayed wild-type (WT)-like plant height, and the three negative lines were similar to *fem3-1*. The three selected positive lines restored 35S::*OsGA2ox1* silencing

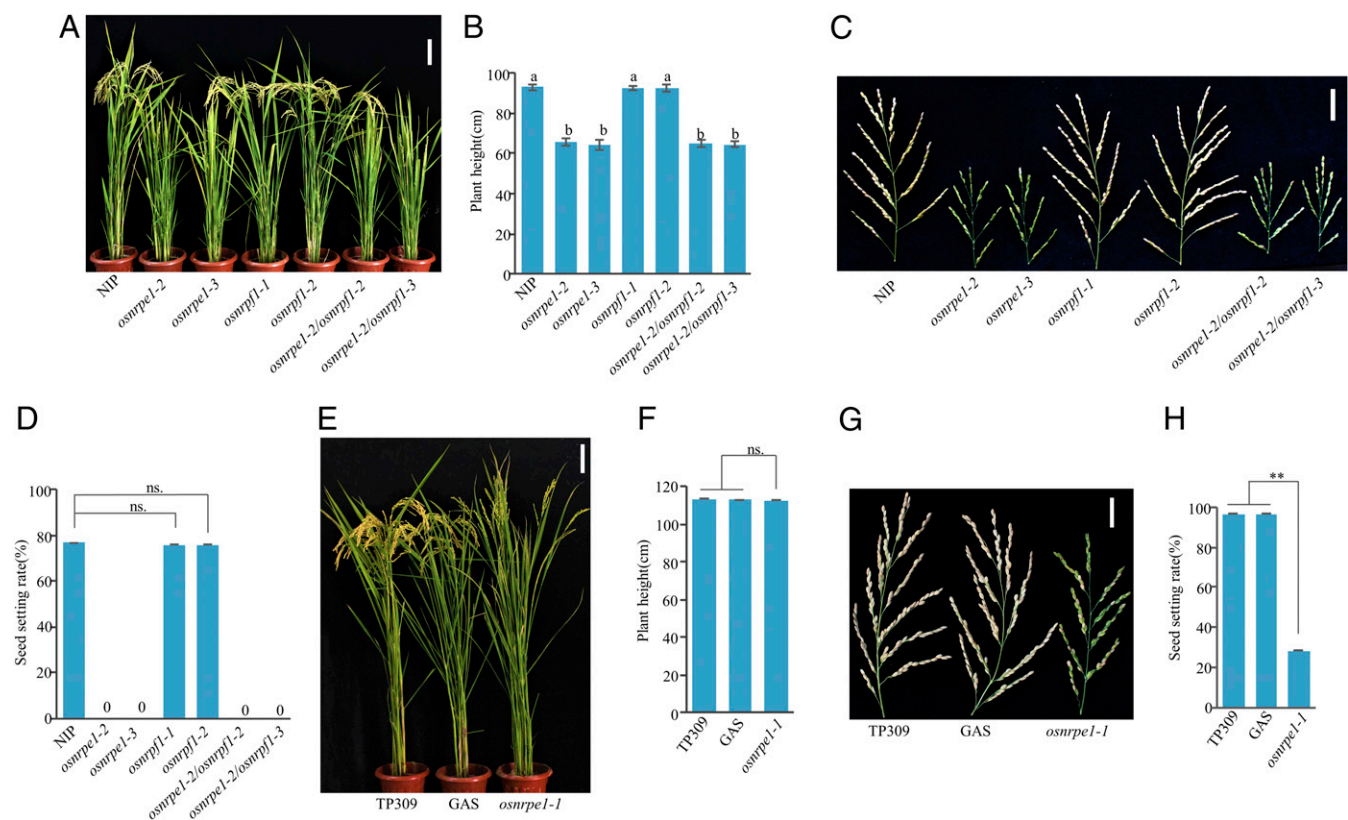


Fig. 2. *OsNRPE1* regulates important agronomic traits. (A) The morphologies of Nipponbare, *osnrpe1*, *osnrpf1*, and *osnrpe1osnrpf1* plants. (Scale bar, 10 cm.) (B) Plant height of the indicated genotypes. Values are means \pm SD; means with different letters are significantly different ($P < 0.05$) according to Fisher's least significant difference (LSD). (C) Seed setting phenotype of the indicated genotypes. (Scale bar, 5 cm.) (D) Seed setting rate in various genotypes ($n = 10$). Values are means \pm SD; ns. indicates that the compared means were not significantly different ($P > 0.05$). (E) Morphologies of TP309, GAS, and *osnrpe1-1* without 35S::*OsGA2ox1*. (Scale bar, 10 cm.) (F) Plant height of TP309, GAS, and *osnrpe1-1* ($n = 10$). Values are means \pm SD; ns. indicates that the compared means were not significantly different ($P > 0.05$). (G) Seed setting phenotype in *osnrpe1-1* and control plants. (Scale bar, 5 cm.) (H) Seed setting rate in *osnrpe1-1* and control plants ($n = 10$). Values are means \pm SD; ** indicates that the compared means are significantly different at $P < 0.01$ according to Student's *t* test.

and plant height (Fig. 1H and *SI Appendix*, Fig. S1 D and E). In addition, the CHH methylation levels at the 35S promoter and at six endogenous loci were also restored in the complemented plants (*SI Appendix*, Fig. S1 F and G). These results demonstrated that mutation in LOC Os02g05880 is responsible for overexpression of *OsGA2ox1* in the *fem3-1* mutant.

Pol V Regulates Important Agronomic Traits. LOC_Os02g05880 encodes the largest subunit of RNA polymerase V, OsNRPE1 (*SI Appendix*, Fig. S2A), and the rice genome contains a homologous gene of *OsNRPE1*, *OsNRPF1* (LOC_Os01g73430) (42, 43) (*SI Appendix*, Fig. S2A). Both OsNRPE1 and OsNRPF1 have A through H domains and a DeCL domain, which are the typical domains of the largest subunit of RNA polymerase (*SI Appendix*, Fig. S2B). The two proteins differ, however, in that the CTD of OsNRPE1 contains five imperfect repeats of 51 amino acids, which are absent in the CTD of OsNRPF1 (*SI Appendix*, Fig. S2B). Because the repeats are required for interaction with AGO4 and DNA methylation in *Arabidopsis* (44, 45), we hypothesized that OsNRPF1 might not be involved in RdDM. The spatiotemporal expression patterns of *OsNRPE1* and *OsNRPF1* were examined by qRT-PCR. Both *OsNRPE1* and *OsNRPF1* were predominately expressed in the inflorescence and anther (*SI Appendix*, Fig. S2C). However, the transcriptional levels were much higher for *OsNRPE1* than for *OsNRPF1* in various tissues (*SI Appendix*, Fig. S2C), suggesting that OsNRPE1 likely functions as the main and largest subunit of Pol V in rice.

Using CRISPR/Cas9 technology, we created *osnrpe1*, *osnrpf1*, and *osnrpe1/osnrpf1* mutants in the Nipponbare background. For *osnrpe1* and *osnrpf1* mutations, one-base insertion or deletion near the protospacer-adjacent motif caused a premature stop codon and a truncated protein (*SI Appendix*, Fig. S2D). Chop-PCR assay showed that the *osnrpe1* and *osnrpe1/osnrpf1* mutants exhibited hypomethylation on six of the tested RdDM loci but that DNA methylation levels in *osnrpf1* single mutants were not reduced (*SI Appendix*, Fig. S2E), suggesting that OsNRPF1 is probably non-functional in mediating DNA methylation.

osnrpe1 and *osnrpe1/osnrpf1* plants but not *osnrpf1* plants were significantly shorter than WT plants (Fig. 2 A and B). In addition, neither *osnrpe1* nor *osnrpe1/osnrpf1* plants produced seeds, while seed setting was normal in *osnrpf1* plants (Fig. 2 C and D). The encoded protein's structure, expression pattern, role in DNA methylation, and effects on plant morphology demonstrate that *OsNRPE1* but not *OsNRPF1* encodes the largest subunit of Pol V in rice. We obtained *osnrpe1-1* (*fem3-1*) without the transgene by backcrossing with TP309 WT plants and segregating out 35S::*OsGA2ox1* in the F2 population. The stature of *osnrpe1-1* plants was quite similar to that of control plants of TP309 and GAS (Fig. 2 E and F); in contrast, *osnrpe1* plants were shorter than WT plants in the Nipponbare background (Fig. 2 A and B). Moreover, *osnrpe1-1* produced some seeds even though its seed setting rate was 70% lower than that of the WT (Fig. 2 G and H). The difference in *osnrpe1* performance in Nipponbare versus TP309 can probably be attributed to the weak allele for *osnrpe1-1* in TP309 and to differences in the genetic background. Overall, the phenotypic analysis of *osnrpe1* mutants in Nipponbare and TP309 indicated that OsNRPE1 but not OsNRPF1 functions as the largest subunit of Pol V and plays a vital role in reproductive development, which is consistent with a previous hypothesis that OsNRPF1 encodes the largest subunit of Pol VI (43).

Pol V Regulates Genome-Wide CHH Methylation. To determine the effect of *OsNRPE1* on the methylome, we performed WGBS on 18-d-old seedlings of *osnrpe1-2*, *osrd2-6*, and Nipponbare. The whole-genome methylation levels of CG and CHG were similar in *osnrpe1-2* and the WT. However, the CHH methylation level was lower in *osnrpe1-2* than in the WT (WT: 3.10%, *osnrpe1-2*: 1.60%) (*SI Appendix*, Fig. S3A and *Dataset S2*). Consistent with

the latter finding, CHH hypomethylated differentially methylated regions (hypo-DMRs) were the dominant DMRs in terms of abundance and length in *osnrpe1-2* (*SI Appendix*, Fig. S3 B and C). About 66.6% of the CHH hypo-DMRs of *osnrpe1-2* were located on transposable elements (TEs) (Fig. 3A). Among the TEs that overlapped with CHH hypo-DMRs, MITEs were the main targets (Fig. 3B), which is quite similar to that in *osrd2* (38). The methylation levels of CG and CHG on both genes and TEs in *osnrpe1-2* were similar to those in the WT (Fig. 3 C and D). The CHH methylation level, however, was substantially lower in *osnrpe1-2* than in the WT, especially on the borders of genes and TEs (Fig. 3 C and D). We divided TEs into six subgroups based on length (<0.5 kb, 0.5 to 1.0 kb, 1.0 to 2.0 kb, 2.0 to 3.0 kb, 3.0 to 4.0 kb, and >4.0 kb) and found that CHH methylation was dependent on *OsNRPE1* and was mainly located on short TEs (Fig. 3E). The dependency of *OsNRPE1* on CHH methylation is reminiscent of *FEM1*, which encodes OsRDR2 (38).

A Venn diagram showed that 75.29% of the CHH hypo-DMRs in *osnrpe1-2* overlapped with those in *osrd2-6* (Fig. 3F). On the *osnrpe1-2*-specific CHH hypo-DMRs, the CHH methylation level was significantly lower in *osrd2-6* than in the WT. On the *osrd2-6*-specific CHH hypo-DMRs, the CHH methylation level was significantly lower in *osnrpe1-2* than in the WT (Fig. 3F), indicating that *OsNRPE1* and *OsRDR2* function together in de novo methylation on RdDM loci in rice.

To determine whether OsNRPE1 is responsible for producing scaffold transcripts in RdDM, we selected six loci (*SI Appendix*, Fig. S4 A and B). On three loci *OsIGN3*, *OsIGN5*, and *OsIGN6*, the transcript levels in the *osnrpe1* mutant were comparable to those in the WT (*SI Appendix*, Fig. S4C). On *OsIGN1*, *OsIGN2*, and *OsIGN4*, the transcripts were largely down-regulated in the *osnrpe1-2* mutant relative to the WT and the *osrd2-6* mutant (Fig. 3G), suggesting that OsNRPE1-dependent transcripts probably function in RdDM.

In TP309, we used CRISPR/Cas9 technology to knockout two *OsNRPD1* genes in order to create the *pol iv* mutants (*SI Appendix*, Fig. S5A). Like the *osnrpe1-1* mutant, the *pol iv* mutants had significantly reduced fertility (*SI Appendix*, Fig. S5 B and C). We then conducted WGBS with 18-d-old seedlings of *osnrpe1-1* (without 35S::*OsGA2ox1*), *pol iv* (*osnrpd1a-1/osnrpd1b-1*), and two types of WT (TP309-replicate 1 was WT, and TP309-replicate 2 was GAS). The whole-genome methylation level of CHH was lower in *osnrpe1-1* than in the WTs (TP309-R1: 2.60%, TP309-R2: 2.40%, *osnrpe1-1*: 1.60%, *pol iv*: 1.70%; *SI Appendix*, Fig. S5D and *Dataset S2*). Consistent with the whole-genome methylation, CHH hypo-DMRs were the main type of DMRs for *osnrpe1-1* and *pol iv* (*SI Appendix*, Fig. S5E). In addition, the total length and number of CHH hypo-DMRs were similar in *osnrpe1-1* and *pol iv* (*SI Appendix*, Fig. S5 E and F). Like in Nipponbare, the majority of CHH hypo-DMRs in *osnrpe1-1* and *pol iv* were located on TEs, and among them, MITEs were major targets (*SI Appendix*, Fig. S5 G and H). The substantially reduced CHH methylation levels in *osnrpe1-1* and *pol iv* suggested that the high CHH methylation on gene borders and TEs was dependent on Pol IV and Pol V (*SI Appendix*, Fig. S5 I and J). The CHH methylation mainly occurred on short TEs, which is also dependent on Pol IV and Pol V (*SI Appendix*, Fig. S5K). More than 79.59% of the CHH hypo-DMRs of *osnrpe1-1* were shared by *pol iv* (*SI Appendix*, Fig. S5L), suggesting that Pol IV and Pol V act together in RdDM in rice. In addition, about 92.39% of the CHH hypo-DMRs of *osnrpe1-1* overlapped with those of *osnrpe1-2* (Fig. 3H), suggesting that RdDM targets are largely conserved in different varieties of rice.

Pol V Controls 24-nt siRNA Accumulation in a Locus-Specific Manner. To understand the role of Pol V in the regulation of 24-nt siRNA accumulation on a genome scale, we performed sRNA-seq with 18-d-old seedlings of *osnrpe1-1*, *osnrpe1-2*, *osrd2-6*, and *pol iv* mutants, and of the WTs of Nipponbare and TP309. More than

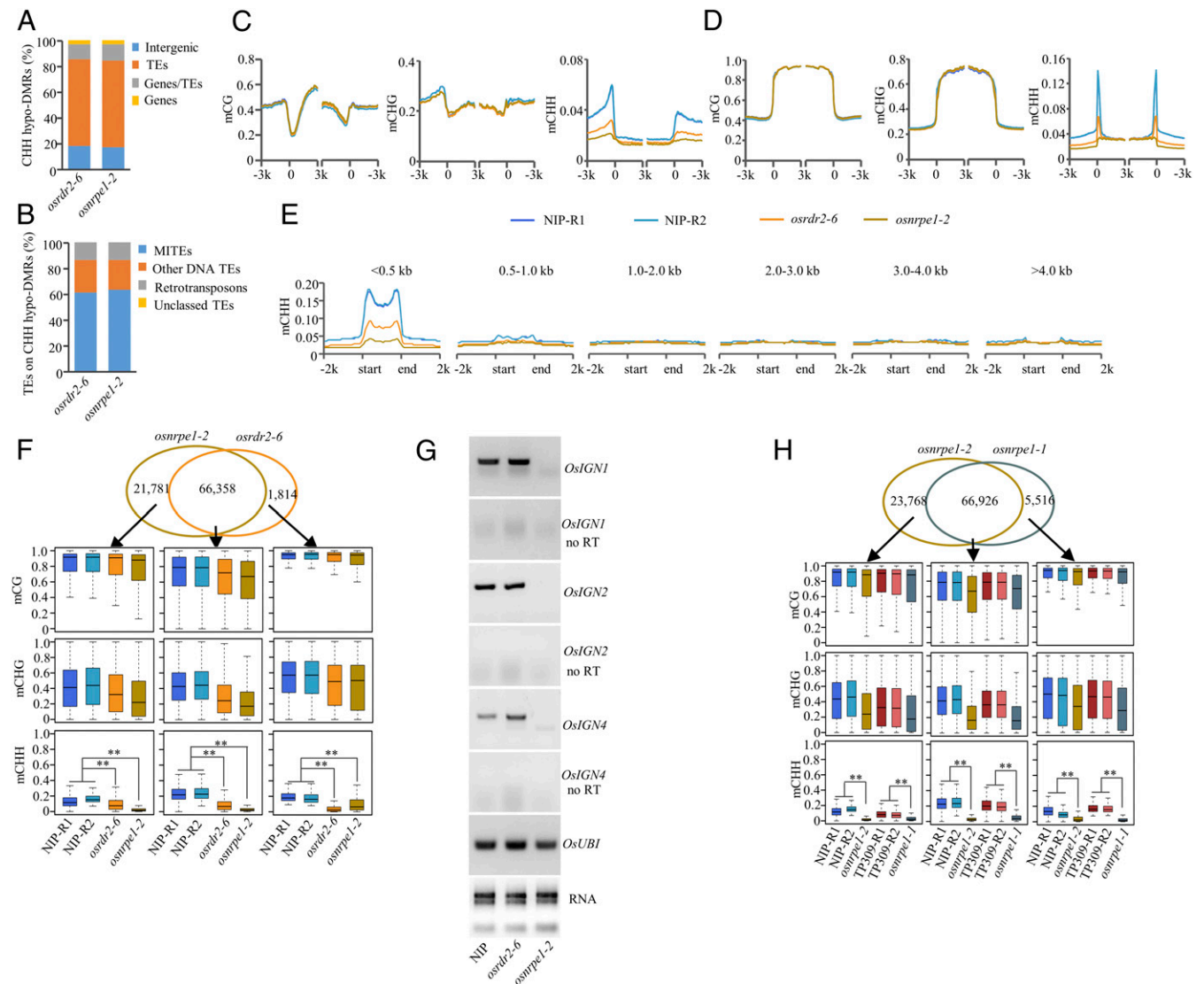


Fig. 3. OsNRPE1 controls genome-wide CHH methylation. (A) Genomic location of CHH hypo-DMRs in *osrd2-6* and *osnrpe1-2*. (B) TE categories associated with CHH hypo-DMRs in *osrd2-6* and *osnrpe1-2*. (C and D) DNA methylation levels of CG, CHG, and CHH on genes (C) and on TEs (D) in Nipponbare, *osrd2-6*, and *osnrpe1-2*. The average methylation levels within each 100-bp interval are plotted. (E) CHH methylation levels on TEs of different lengths in Nipponbare, *osrd2-6*, and *osnrpe1-2*. (F, Top) Venn diagram showing the overlap of CHH hypo-DMRs in *osrd2-6* and *osnrpe1-2*. (Bottom) DNA methylation levels of CG, CHG, and CHH in the indicated genotypes on *osrd2-6*-specific, *osnrpe1-2*-specific, and overlapped CHH hypo-DMRs as indicated by box plots. ** indicates that compared plots are significantly different at $P < 0.01$ (Fisher's LSD). (G) RT-PCR analysis of Pol V-dependent transcripts on loci *OsIGN1*, *OsIGN2*, and *OsIGN4* in Nipponbare and in the *osrd2-6* and *nrpe1-2* mutants. (H, Top) Venn diagram showing the overlap of CHH hypo-DMRs in *osnrpe1-2* and *osnrpe1-1*. (Bottom) DNA methylation levels of CG, CHG, and CHH on *osnrpe1-2*-specific, *osnrpe1-1*-specific, and overlapped CHH hypo-DMRs as indicated by box plots. ** indicates that compared plots are significantly different at $P < 0.01$ (Fisher's LSD).

20 million raw reads were obtained for each of the genotypes (Dataset S2). After low quality reads and the structural RNA were removed, the clean sRNA reads were mapped to the rice genome (RGAP7.0). The abundance of 24-nt siRNAs was calculated using the reads per ten million mapped reads (RPTM) normalized by all unique mapped reads. In the Nipponbare background, the accumulation of 24-nt siRNAs was substantially reduced in *osrd2-6* and moderately reduced in *osnrpe1-2* (Fig. 4A). In the TP309 background, the accumulation of 24-nt siRNAs was almost eliminated in *pol iv* but was only slightly decreased in *osnrpe1-1* (Fig. 4A).

We merged the 24-nt siRNAs within 100-base pair (100-bp) windows, and the loci with an RPTM value >12 were defined as 24-nt siRNA clusters. A total of 57,644 24-nt siRNA clusters were defined in the Nipponbare WT, but only 4,951 siRNA

clusters were defined in the *osrd2-6* mutant (Fig. 4B). The *osnrpe1-2* mutant, however, retained a majority of the siRNA clusters of the WT (Fig. 4B). We defined 47,445 24-nt siRNA clusters in the TP309 WT and only 2,068 in the *pol iv* mutant (Fig. 4B). Again, *osnrpe1-1* retained most of the siRNA clusters of the WT (Fig. 4B). These results suggested that 24-nt siRNA production is fully dependent on OsRDR2 and Pol IV but only partially dependent on Pol V in rice. Interestingly, *osnrpe1-1* generated 8,928 new 24-nt siRNA clusters in the TP309 background, and *osnrpe1-2* generated 5,738 new 24-nt siRNA clusters in the Nipponbare background (Fig. 4B). We then combined the 24-nt siRNA clusters in the WT and mutants in the same genetic background. We obtained 63,947 24-nt siRNA clusters in Nipponbare and 57,044 in TP309. The combined 24-nt siRNA clusters in the same genetic background were divided into six subsets based

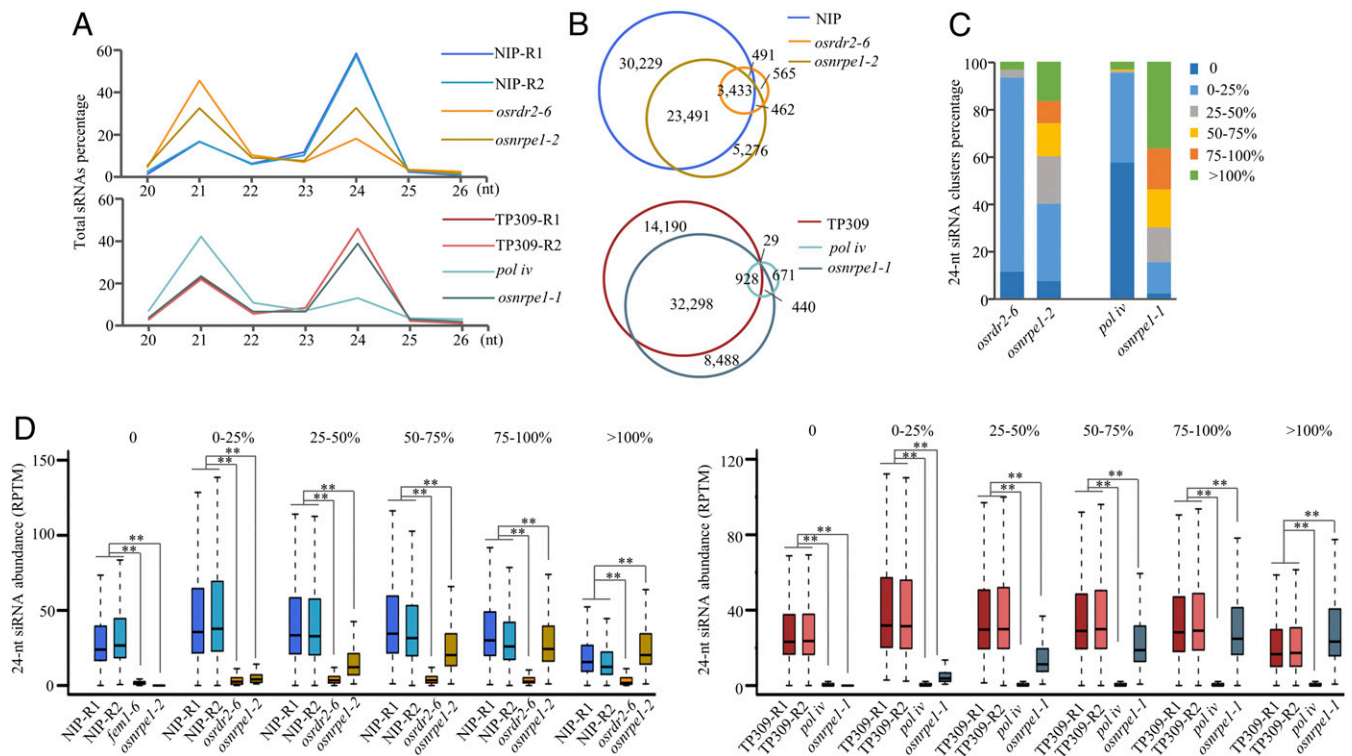


Fig. 4. The accumulation of 24-nt siRNA partially depends on *OsNRPE1* in rice. (A) Size distribution of sRNAs in Nipponbare, *osrd2-6*, and *osnrpe1-2* (Upper), and in TP309, *pol iv*, and *osnrpe1-1* (Lower). (B) Venn diagram indicating 24-nt siRNA cluster numbers and their overlap in Nipponbare, *osrd2-6*, and *osnrpe1-2* (Upper) or in TP309, *pol iv*, and *osnrpe1-1* (Lower). (C) Ratios of 24-nt siRNA clusters in different groups based on the abundance in the mutant relative to that in the WT. (D) Abundance of 24-nt siRNAs in the indicated genotypes in six subsets of 24-nt siRNA clusters as indicated by box plots. ** indicates that compared plots are significantly different at $P < 0.01$ (Fisher's LSD).

on the ratio of siRNA abundance in mutants compared to that in the WT (0, 0 to 25%, 25 to 50%, 50 to 75%, 75 to 100%, and >100%; *SI Appendix, Fig. S6*). In the Nipponbare background, more than 93% of the 24-nt siRNA clusters belonged to 0 and 0 to 25% subsets in *osrd2-6*; however, only 40% belonged to the same subsets in *osnrpe1-2* (Fig. 4C). In *pol iv*, about 96% of 24-nt siRNA clusters had siRNA abundances that were <25% of that in the WT background of TP309. However, only about 16% of 24-nt siRNA clusters in *osnrpe1-1* had siRNA abundances that were <25% compared to the TP309 WT (Fig. 4C).

As illustrated by the box plots of the six subsets of 24-nt siRNA clusters in the *osnrpe1* mutant, almost all of the 24-nt siRNAs were eliminated in *osrd2-6* and *pol iv* (Fig. 4D), suggesting that 24-nt siRNA biogenesis is fully dependent on OsRDR2 and Pol IV. The accumulation of siRNAs in *osnrpe1* was eliminated, partially lost, fully retained, or even increased in a subset-specific manner in both backgrounds (Fig. 4D). Together, the results indicate that the accumulation of 24-nt siRNAs is fully dependent on OsRDR2 and Pol IV but partially dependent on Pol V.

DNA Methylation Is Required for 24-nt siRNA Accumulation on Pol V-Dependent Loci. Total cytosine methylation levels and CG, CHG, and CHH methylation levels were significantly reduced in all subsets of 24-nt siRNA clusters in *osnrpe1-1* and *osnrpe1-2* except CG methylation in the 75 to 100% and >100% subsets in *osnrpe1-2* (*SI Appendix, Fig. S7A and B*). For total C, CG, CHG, and CHH contexts, the reduction of methylation levels in *osnrpe1* relative to the WT gradually declined from OsNRPE1 fully dependent 24-nt siRNA clusters to OsNRPE1 fully independent 24-nt siRNA clusters in both Nipponbare and TP309 backgrounds (Fig. 5A). In addition, the methylation reduction pattern in *osrd2* and *pol iv* was similar to that in *osnrpe1* (*SI Appendix, Fig. S7C*

and D), suggesting that RdDM is more important for maintaining DNA methylation in subsets of 24-nt siRNA clusters that depend on Pol V than in subsets of 24-nt siRNA clusters that do not depend on Pol V.

Based on the relationship between OsNRPE1-affected DNA methylation and OsNRPE1-affected siRNA clusters, we hypothesized that the DNA methylation features may be involved in the effect of OsNRPE1 on 24-nt siRNA accumulation. We analyzed the methylation levels in the three DNA sequence contexts of the six subsets of 24-nt siRNA clusters of *osnrpe1* mutants in WT plants and found that the CG and CHG methylation levels gradually increased from OsNRPE1 fully dependent subsets of 24-nt siRNA clusters to OsNRPE1 fully independent subsets in both Nipponbare and TP309 backgrounds (Fig. 5B). The pattern in the CHH context was opposite to that in the CG and CHG contexts; that is, the methylation level in the CHH context progressively decreased from 24-nt siRNA clusters that were fully dependent on Pol V to 24-nt siRNA clusters that were fully independent of Pol V (Fig. 5B). For total cytosine methylation levels in the Nipponbare background, in contrast, the methylation levels did not display the trend displayed by CG, CHG, and CHH (*SI Appendix, Fig. S7E*). The methylation level of total cytosine in the 0% subset of 24-nt siRNA clusters, however, was significantly lower than in other subsets of 24-nt siRNA clusters in the Nipponbare background (*SI Appendix, Fig. S7E*). In the TP309 background, the methylation levels of all cytosine in the subsets of 0 and 0 to 25% of 24-nt siRNA clusters were significantly lower than those in other subsets of 24-nt siRNA clusters (*SI Appendix, Fig. S7E*). Together, these results demonstrate that 24-nt siRNA accumulation on loci with higher CHH methylation levels and lower CG and CHG methylation levels tends to be more dependent on Pol V than 24-nt siRNA

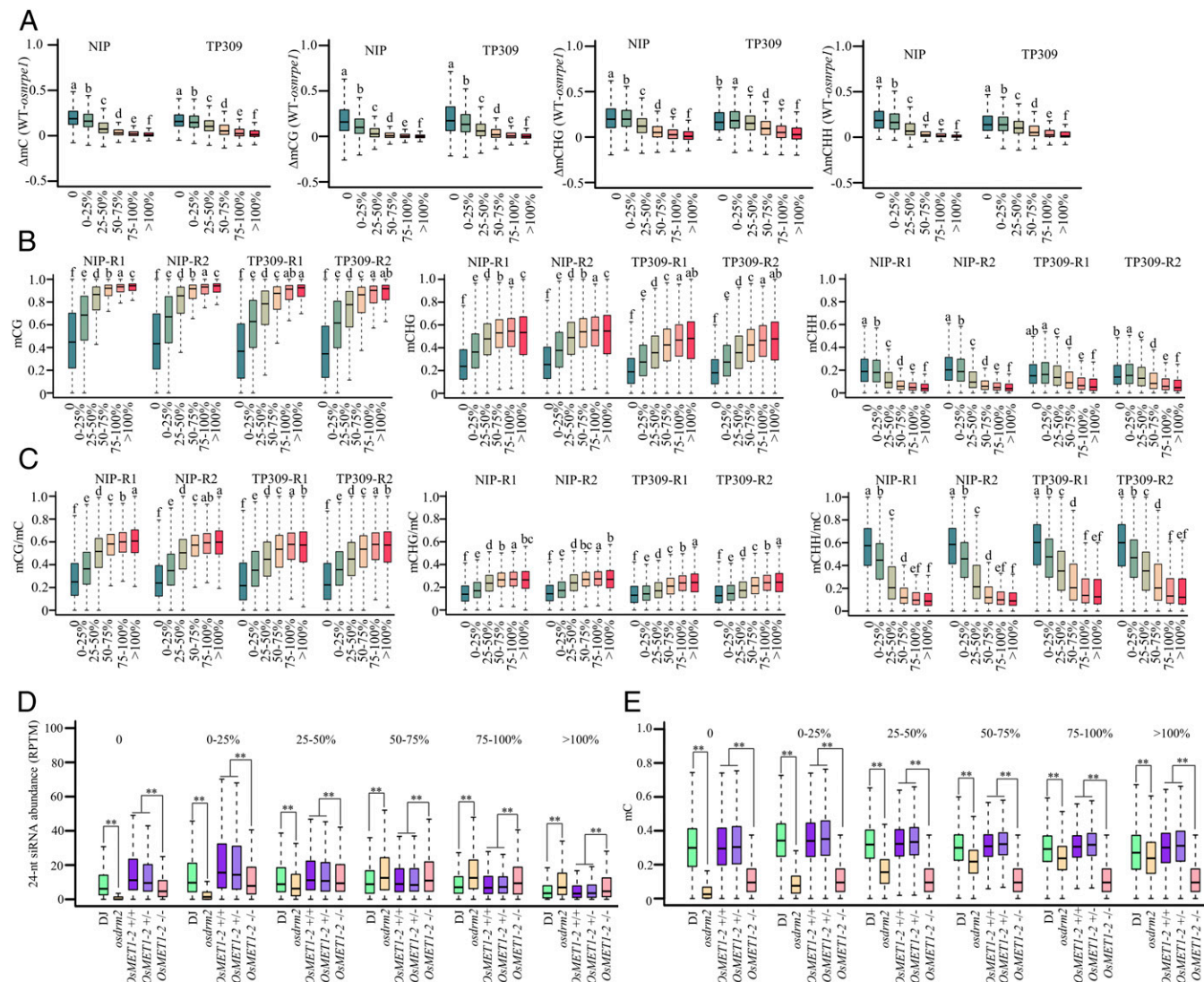


Fig. 5. DNA methylation context affects the dependency of 24-nt siRNA accumulation on Pol V. (A) Reduction in methylation levels for the *osnrpe1* mutant relative to the WT in total cytosine, CG, CHG, and CHH in six subsets of 24-nt siRNA clusters in backgrounds of Nipponbare and TP309. (B) DNA methylation levels of CG, CHG, and CHH in six subsets of 24-nt siRNA clusters in WT of Nipponbare and TP309. (C) Ratios of mCG/mC, mCHG/mC, and mCHH/mC in total methylated cytosine in six subsets of 24-nt siRNA clusters in backgrounds of Nipponbare and TP309. (D) Abundance of 24-nt siRNAs in the indicated genotypes in six subsets of 24-nt siRNA clusters of *osnrpe1-2* as indicated by box plots. (E) Total cytosine methylation levels in the indicated genotypes in six subsets of 24-nt siRNA clusters of *osnrpe1-2* as indicated by box plots. Within each of the two or four groups of six box plots in each panel, plots with different letters are significantly different at $P < 0.05$ according to Fisher's LSD. ** indicates that compared plots are significantly different at $P < 0.01$ (Fisher's LSD).

accumulation on loci with higher CG and CHG methylation levels and lower CHH methylation levels.

In addition, the ratio of mCG/mC and mCHG/mC gradually increased from 24-nt siRNA clusters that were fully dependent on Pol V to 24-nt siRNA clusters that were fully independent of Pol V (Fig. 5C). The ratio of mCHH/mC, however, gradually decreased from 24-nt siRNA clusters that were fully dependent on Pol V to 24-nt siRNA clusters that were fully independent of Pol V (Fig. 5C). For all cytosines, the contents of CG and CHG increased, but the content of CHH decreased from 24-nt siRNA clusters that were fully dependent on Pol V to 24-nt siRNA clusters that were fully independent of Pol V (SI Appendix, Fig. S7F). The trend of cytosine content throughout different subsets of 24-nt siRNA clusters was similar to that of methylated cytosine content (Fig. 5C and SI Appendix, Fig. S7F). Overall, the GC content was lower on Pol V-dependent 24-nt siRNA clusters than on Pol V-independent 24-nt siRNA clusters in both backgrounds (SI Appendix, Fig. S7G).

Furthermore, 24-nt siRNA clusters that were fully dependent on Pol V were shorter than clusters that were fully independent of Pol V (SI Appendix, Fig. S7H), indicating that the features of DNA sequence might regulate the dependency of 24-nt siRNA biogenesis on Pol V.

To evaluate whether DNA methylation determines the dependency of 24-nt siRNA accumulation on Pol V, we first analyzed the siRNAs and methylome of the *osdrm2* mutant (46, 47). On Pol V fully dependent loci, siRNA accumulation was almost totally eliminated in the *osdrm2* mutant. On Pol V fully independent loci, by contrast, siRNA abundance was greater in the *osdrm2* mutant than in the WT (Fig. 5D). The dependency of siRNA accumulation on OsDRM2 was similar to that on Pol V. Total cytosine methylation levels and CG, CHG, and CHH methylation levels were significantly reduced in all subsets of 24-nt siRNA clusters in the *osdrm2* mutant (Fig. 5E and SI Appendix, Fig. S8A). For total C, CG, CHG, and CHH contexts, the reduction of methylation

levels in *osdrm2* relative to the WT gradually declined from Pol V fully dependent 24-nt siRNA clusters to Pol V fully independent 24-nt siRNA clusters (*SI Appendix, Fig. S8B*), which is also similar to that in *osnrpe1*, *osrd2*, and *pol iv* mutants.

We next analyzed siRNAs and the methylome in the *osmet1-2* mutant in which the majority of CG methylation is lost (48). Total cytosine methylation level and CG, CHG, and CHH methylation levels were significantly reduced in all subsets of 24-nt siRNA clusters in the *osmet1-2* mutant (Fig. 5E and *SI Appendix, Fig. S8 A and B*). In subsets of 0, 0 to 25%, and 25 to 50%, the siRNA abundance in *osmet1-2* mutant was significantly lower than in the WT or the heterozygote. In subsets of 50 to 75%, 75 to 100%, and >100%, by contrast, siRNA abundance was significantly higher in the *osmet1-2* mutant than in the WT or the heterozygote (Fig. 5D). Overall, on Pol V–dependent loci, DNA methylation is required for siRNA accumulation.

Histone Modifications Are Associated with 24-nt siRNAs Accumulation on Pol V–Independent Loci. To determine whether other epigenetic marks regulate 24-nt siRNA production on Pol V–independent loci, we analyzed various histone modifications in the six subsets of 24-nt siRNA clusters. The levels of two repressive epigenetic marks, H3K9me1 and H3K9me2, gradually increased from 24-nt siRNA clusters that were fully dependent on Pol V to clusters that were fully independent of Pol V (Fig. 6A). The levels of another repressive epigenetic mark, H3K27me3, gradually decreased from 24-nt siRNA clusters that were fully dependent on Pol V to clusters that were fully independent of Pol V in the Nipponbare but not in the TP309 background (Fig. 6A), suggesting that Pol V–independent clusters tend to locate on stable but not conditional heterochromatin. In contrast, the active epigenetic marks H3K4me2, H3K4ac, H3K9ac, H3K27ac, and H4K16ac gradually decreased from 24-nt siRNA clusters that were fully dependent on Pol V to clusters that were fully independent of Pol V (Fig. 6B). The nucleosome occupancy slightly increased from 24-nt siRNA clusters that were fully dependent on Pol V to clusters that were fully independent of Pol V (Fig. 6C). Consequently, the messenger RNA (mRNA) levels of genes adjacent to 24-nt siRNA clusters were gradually decreased from clusters that were fully dependent on Pol V to clusters that were fully independent of Pol V in both seedlings and panicles (Fig. 6D). These results indicate that repressive histone modifications of H3K9me1 and H3K9me2 likely recruit Pol IV–RDR2 to produce 24-nt siRNAs on Pol V–independent loci.

To study the distribution of 24-nt siRNA clusters in the genome, we inspected chromosome 1 and chromosome 4 on which the representative heterochromatic regions are concentrated in the typical regions (46). For simplicity, we combined three Pol V–dependent 24-nt siRNA clusters (0, 0 to 25%, and 25 to 50%) into a <50% subgroup and three Pol V–independent 24-nt siRNA clusters (50 to 75%, 75 to 100%, and >100%) into a >50% subgroup. On heterochromatic regions, cluster numbers were similar for the two groups. On the euchromatic regions, in contrast, the number of 24-nt siRNA clusters was greater in the <50% subgroup than in the >50% subgroup (*SI Appendix, Fig. S9*). Together, these results suggested that heterochromatin and euchromatin environments are correlated with the dependence of 24-nt siRNA biosynthesis on Pol V.

Discussion

RdDM Is Essential for Reproductive Development in Rice. The RdDM mechanism has been well studied in *Arabidopsis*, but the mutants of most RdDM genes have no obvious developmental defects in *Arabidopsis* (1–9). In other plant species, like maize, tomato, *B. rapa*, and *Capsella rubella*, RdDM mutants display pleiotropic developmental phenotypes, particularly for traits related to reproduction (7–9, 36, 37, 49–54). In rice, mutations in *OsDCL3*, *OsDRM2*, or *OsNRDP1* change important agricultural traits, such as plant stature, flag leaf angle, tiller number, and fertility (39, 40,

46, 55, 56). Recent research demonstrated that maternal Pol IV–dependent siRNAs control seed development by regulating the expression of imprinting genes in *Arabidopsis* (57).

Here, we provided evidence that the mutation of *OsNRPE1* (*FEM3*) fully blocked seed setting in the Nipponbare background and greatly reduced seed setting in the TP309 background (Fig. 2C, D, G, and H). The role of *OsNRPE1* (*FEM3*) in reproductive development is consistent with our previous work with *OsRDR2* (*FEM1*), the mutation of which disrupted both male and female reproductive development and finally resulted in sterility (38). In the current study, the *pol iv* mutant in the TP309 background that was created by mutating two *OsNRPD1* genes also had greatly reduced seed setting (*SI Appendix, Fig. S5 A–C*). The predominant expression of *OsRDR2* (*FEM1*), *OsNRPE1* (*FEM3*), and *OsNRPD1* in reproductive tissues and the reproductive defects in *osrd2* (*fem1*), *osnrpe1* (*fem3*), and *pol iv* mutants demonstrate the important role of RdDM in reproductive development in rice.

Most species of Poaceae have two homologous *NRPE1* genes (42, 43). In the current study with rice, we investigated the homologous gene of *OsNRPE1* (*FEM3*), *OsNRPF1*, which lacks the heptad repeats at the C terminus that are required for interaction with AGO4 and for mediated DNA methylation in *Arabidopsis* (44, 45). We found that the mRNA level is much lower for *OsNRPF1* than *OsNRPE1* (*FEM3*) and that the mutation in *OsNRPF1* does not result in any visible developmental defects. In addition, our Chop-PCR assay indicated that *OsNRPF1* is not involved in DNA methylation. Thus, only *OsNRPE1* encodes the largest subunit of Pol V in rice, and the function of *OsNRPF1* remains unknown (43).

Gene Silencing for 35S::OsGA2ox1. The 35S promoter and *OsGA2ox1* produced abundant 21- and 22-nt siRNAs but few 24-nt siRNAs in GAE. Consequently, DNA methylation on the 35S promoter and *OsGA2ox1* was established, suggesting that noncanonical RdDM or moderate posttranscriptional gene silencing (PTGS) likely occurs in GAE. In GAS, by contrast, 21- and 22-nt siRNAs were absent on both the 35S promoter and *OsGA2ox1*. On the 35S promoter, 24-nt siRNAs were more abundant in GAS than in GAE. These results demonstrated that noncanonical RdDM or moderate PTGS for 35S::*OsGA2ox1* in GAE changed into TGS in GAS, which is similar to the phase transition of epigenetic silencing for other transgenes or TEs (58). The 24-nt siRNAs increased on the 35S promoter but disappeared on *OsGA2ox1* in GAS. From GAE to GAS, the change in the abundance of 24-nt siRNAs and non-CG methylation was opposite on the 35S promoter versus *OsGA2ox1*. The underlying mechanism for the difference warrants additional research.

24-nt siRNAs and DNA Methylation Form a Self-Reinforcing Loop on Euchromatic RdDM Loci. During the initiation and establishment of RdDM, all cytosines including CG, CHG, and CHH are methylated by DRM2. Plants have specific mechanisms to ensure the maintenance of CG and CHG methylation. After DNA replication, however, DNA in the CHH context must be de novo methylated in the newly synthesized strand. The maintenance of CHH methylation is carried out by RdDM and CMT2 in *Arabidopsis* (59). The enrichment of H3K9me1 and H3K9me2 and the nucleosome is lower on Pol V–dependent loci than on Pol V–independent loci (*SI Appendix, Fig. S10*). In contrast, the enrichment of active histone marks is higher on loci with 24-nt siRNAs that are fully dependent on Pol V than on loci with 24-nt siRNAs that are fully independent of Pol V. We propose that Pol V–dependent and –independent 24-nt siRNA clusters belong to the euchromatic and heterochromatic RdDM loci, respectively. On euchromatic loci, DNA methylation in different contexts is interdependent, and DNA methylation in all contexts but not H3K9me2 recruits Pol IV–RDR2 and Pol V to catalyze DNA methylation. siRNA production and the establishment and maintenance of DNA methylation form a positive

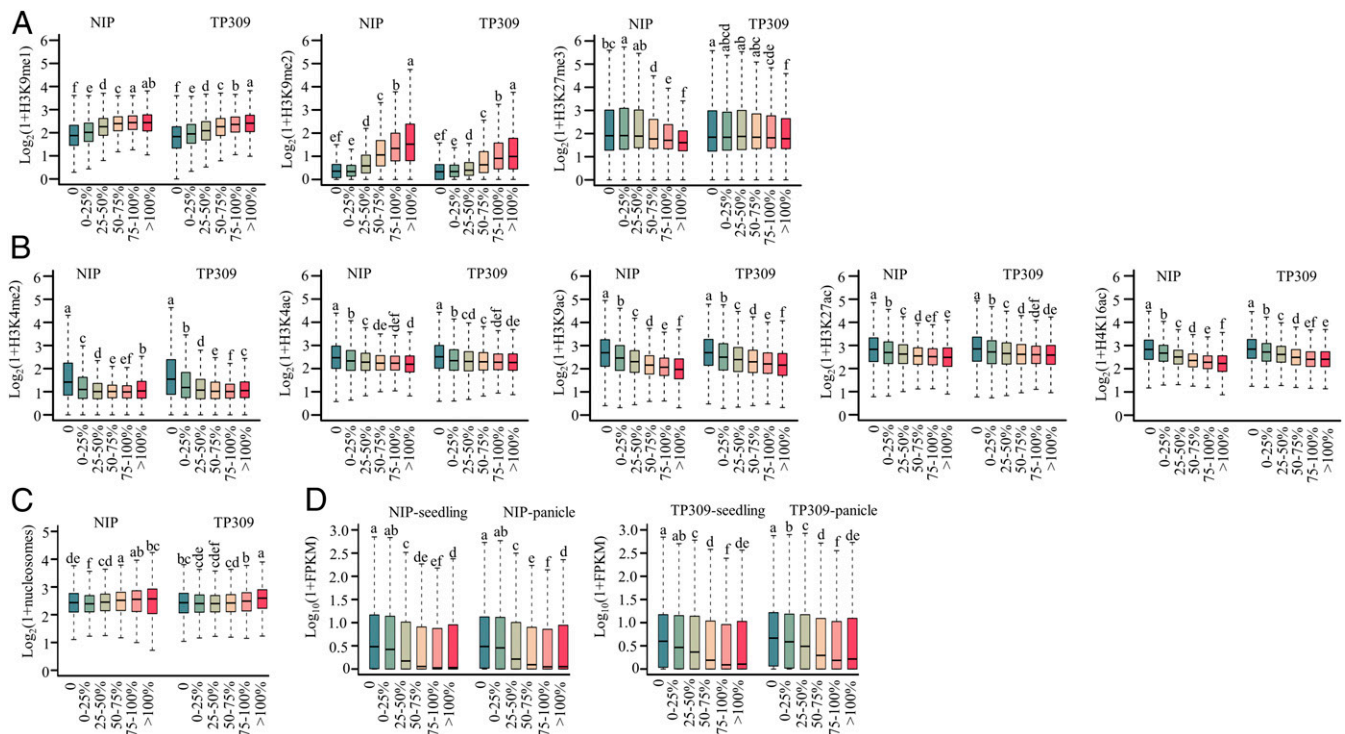


Fig. 6. Histone modifications, nucleosome occupancy, and transcriptional levels in six subsets of 24-nt siRNA clusters. (A) Relative enrichment of repressive histone modifications (H3K9me1, H3K9me2, and H3K27me3) in six subsets of 24-nt siRNA clusters in backgrounds of Nipponbare and TP309. (B) Relative enrichment of active histone modifications (H3K4me2, H3K4ac, H3K9ac, H3K27ac, and H4K16ac) in six subsets of 24-nt siRNA clusters in backgrounds of Nipponbare and TP309. (C) Nucleosome occupancy in six subsets of 24-nt siRNA clusters in backgrounds of Nipponbare and TP309. (D) Transcriptional levels of genes associated with 24-nt siRNA clusters within six subsets in backgrounds of Nipponbare and TP309. Within each of the two groups of six box plots in each panel, plots with different letters are significantly different at $P < 0.05$ according to Fisher's LSD.

feedback loop. On heterochromatic loci, histone modifications like H3K9me2 but not DNA methylation are the main signals that recruit Pol IV-RDR2 to produce 24-nt siRNAs.

Possible Mechanisms Underlying Pol V Repression of siRNA Accumulation.

In addition, we found that *nipe1* mutants contained 5,738 and 8,928 more 24-nt siRNA clusters than the WT in the background of Nipponbare and TP309, respectively (Fig. 4B). Mutation in *OsDRM2* and *OsMET1-2* also increased 24-nt siRNA abundance on Pol V-independent loci. On those loci, the depletion of Pol V or *OsDRM2* might increase chromatin access to Pol IV-OsRDR2 or Pol II-OsRDR6, which function in generating siRNAs. Another possibility is that a reduction in DNA methylation in RdDM mutants or *osmet1-2* likely enhances the recruitment of Pol IV-OsRDR2 or Pol II-OsRDR6, thereby increasing 24-nt siRNA accumulation. Future study of siRNA profiles in mutants associated with Pol V (i.e., *OsAGO4*, *OsIDN2*, *OsKTF1*, *OsDRD1*, *OsDMS3*, and *OsRDM1*) is needed to clarify the repressive role of Pol V on siRNA production. Chromatin immunoprecipitation-sequencing (ChIP-seq) analysis of Pol IV, OsRDR2, Pol II, OsRDR6, nucleosomes, and histone modifications like H3K9me2 in the mutants with increased siRNA production is needed to determine the mechanism by which Pol V, *OsDRM2*, and *OsMET1* repress siRNA production. Determining the effect of Pol V, *OsDRM2*, and *OsMET1* on the chromatin superstructure by Hi-C analysis will also increase our understanding of how Pol V represses 24-nt siRNA accumulation.

1. H. Zhang, J. K. Zhu, RNA-directed DNA methylation. *Curr. Opin. Plant Biol.* **14**, 142–147 (2011).
2. M. A. Matzke, R. A. Mosher, RNA-directed DNA methylation: An epigenetic pathway of increasing complexity. *Nat. Rev. Genet.* **15**, 394–408 (2014).

Materials and Methods

SI Appendix, SI Materials and Methods contains descriptions of performed experiments, including materials and growth conditions, genetic screen of five elements mountain mutants, map-based cloning of *FEM3*, phylogenetic analysis, RNA isolation and analysis of transcriptional levels, DNA methylation analyses of individual loci, and vector construction and plant transformation. It also includes descriptions of data analysis, including whole-genome bisulfite data analysis, sRNA-seq analysis, analysis of ChIP-seq, and gene expression analysis.

Data Availability. The following were uploaded to the National Center for Biotechnology Information (NCBI) Gene Expression Omnibus (GEO) in our previous study (GEO: [GSE130168](https://www.ncbi.nlm.nih.gov/geo/query/acc.cgi?acc=GSE130168)): the bisulfite-seq datasets of Nipponbare and *fem1-6* (*osrdr2-6*); the sRNA-seq datasets of Nipponbare, *fem1-6*, and TP309; and the RNA-seq datasets of Nipponbare and TP309. The following were uploaded to the NCBI GEO in the current study (GEO: [GSE158711](https://www.ncbi.nlm.nih.gov/geo/query/acc.cgi?acc=GSE158711)): the bisulfite-seq datasets of TP309, *GAS*, *pol iv*, *fem3-1* (*osnrpe1-1*), and *fem3-2* (*osnrpe1-2*) and the sRNA-seq datasets of *pol iv*, *fem3-1* (*osnrpe1-1*), and *fem3-2* (*osnrpe1-2*). The following data were downloaded from NCBI: the bisulfite-seq and sRNA-seq datasets of DJ and *osdrm2* (GEO: [GSE81436](https://www.ncbi.nlm.nih.gov/geo/query/acc.cgi?acc=GSE81436)) (46) and of Nipponbare and *osmet1-2* ([SRP043447](https://www.ncbi.nlm.nih.gov/geo/query/acc.cgi?acc=SRP043447), [SRP043449](https://www.ncbi.nlm.nih.gov/geo/query/acc.cgi?acc=SRP043449)) (48). All other study data are included in the article and/or supporting information.

ACKNOWLEDGMENTS. This study was supported by the National Natural Science Foundation of China (31671340), the Natural Science Foundation of Jiangsu Province (BK20170027), and the Jiangsu Collaborative Innovation Center for Modern Crop Production to D.-L.Y. The high-throughput sequencing data were analyzed on the high-performance computing platform of the Bioinformatics Center, Nanjing Agricultural University.

3. J. M. Wendte, C. S. Pikaard, The RNAs of RNA-directed DNA methylation. *Biochim. Biophys. Acta. Gene Regul. Mech.* **1860**, 140–148 (2017).
4. M. A. Matzke, T. Kanno, A. J. Matzke, RNA-directed DNA methylation: The evolution of a complex epigenetic pathway in flowering plants. *Annu. Rev. Plant Biol.* **66**, 243–267 (2015).

5. R. M. Erdmann, C. L. Picard, RNA-directed DNA methylation. *PLoS Genet.* **16**, e1009034 (2020).
6. H. Zhang, J. K. Zhu, New discoveries generate new questions about RNA-directed DNA methylation in *Arabidopsis*. *Natl. Sci. Rev.* **4**, 10–15 (2017).
7. B. Rymen, L. Ferrafiat, T. Blevins, Non-coding RNA polymerases that silence transposable elements and reprogram gene expression in plants. *Transcription* **11**, 172–191 (2020).
8. H. T. Chow, T. Chakraborty, R. A. Mosher, RNA-directed DNA Methylation and sexual reproduction: Expanding beyond the seed. *Curr. Opin. Plant Biol.* **54**, 11–17 (2020).
9. R. Wambui Mbichi, Q. F. Wang, T. Wan, RNA directed DNA methylation and seed plant genome evolution. *Plant Cell Rep.* **39**, 983–996 (2020).
10. L. M. Smith *et al.*, An SNF2 protein associated with nuclear RNA silencing and the spread of a silencing signal between cells in *Arabidopsis*. *Plant Cell* **19**, 1507–1521 (2007).
11. H. Zhang *et al.*, DTF1 is a core component of RNA-directed DNA methylation and may assist in the recruitment of Pol IV. *Proc. Natl. Acad. Sci. U.S.A.* **110**, 8290–8295 (2013).
12. J. A. Law *et al.*, Polymerase IV occupancy at RNA-directed DNA methylation sites requires SHH1. *Nature* **498**, 385–389 (2013).
13. D. L. Yang *et al.*, Four putative SWI2/SNF2 chromatin remodelers have dual roles in regulating DNA methylation in *Arabidopsis*. *Cell Discov.* **4**, 55 (2018).
14. M. Zhou, A. M. S. Palanca, J. A. Law, Locus-specific control of the de novo DNA methylation pathway in *Arabidopsis* by the CLASSY family. *Nat. Genet.* **50**, 865–873 (2018).
15. T. Blevins *et al.*, Identification of Pol IV and RDR2-dependent precursors of 24 nt siRNAs guiding de novo DNA methylation in *Arabidopsis*. *eLife* **4**, e09591 (2015).
16. J. Zhai *et al.*, A one precursor one siRNA model for Pol IV-dependent siRNA biogenesis. *Cell* **163**, 445–455 (2015).
17. R. Ye *et al.*, A dicer-independent route for biogenesis of siRNAs that direct DNA methylation in *Arabidopsis*. *Mol. Cell* **61**, 222–235 (2016).
18. D. L. Yang *et al.*, Dicer-independent RNA-directed DNA methylation in *Arabidopsis*. *Cell Res.* **26**, 66–82 (2016).
19. J. Singh, V. Mishra, F. Wang, H. Y. Huang, C. S. Pikaard, Reaction mechanisms of Pol IV, RDR2, and DCL3 drive RNA channeling in the siRNA-directed DNA methylation pathway. *Mol. Cell* **75**, 576–589.e5 (2019).
20. J. R. Haag *et al.*, In vitro transcription activities of Pol IV, Pol V, and RDR2 reveal coupling of Pol IV and RDR2 for dsRNA synthesis in plant RNA silencing. *Mol. Cell* **48**, 181–188 (2012).
21. Z. Xie *et al.*, Genetic and functional diversification of small RNA pathways in plants. *PLoS Biol.* **2**, E104 (2004).
22. S. Mi *et al.*, Sorting of small RNAs into *Arabidopsis* argonaute complexes is directed by the 5' terminal nucleotide. *Cell* **133**, 116–127 (2008).
23. A. T. Wierzbicki, J. R. Haag, C. S. Pikaard, Noncoding transcription by RNA polymerase Pol IVb/Pol V mediates transcriptional silencing of overlapping and adjacent genes. *Cell* **135**, 635–648 (2008).
24. A. T. Wierzbicki, T. S. Ream, J. R. Haag, C. S. Pikaard, RNA polymerase V transcription guides ARGONAUTE4 to chromatin. *Nat. Genet.* **41**, 630–634 (2009).
25. X. Zhong *et al.*, Molecular mechanism of action of plant DRM de novo DNA methyltransferases. *Cell* **157**, 1050–1060 (2014).
26. X. Zhong *et al.*, DDR complex facilitates global association of RNA polymerase V to promoters and evolutionarily young transposons. *Nat. Struct. Mol. Biol.* **19**, 870–875 (2012).
27. L. M. Johnson *et al.*, SRA- and SET-domain-containing proteins link RNA polymerase V occupancy to DNA methylation. *Nature* **507**, 124–128 (2014).
28. Z. W. Liu *et al.*, The SET domain proteins SUVH2 and SUVH9 are required for Pol V occupancy at RNA-directed DNA methylation loci. *PLoS Genet.* **10**, e1003948 (2014).
29. M. Tsuzuki *et al.*, Broad noncoding transcription suggests genome surveillance by RNA polymerase V. *Proc. Natl. Acad. Sci. U.S.A.* **117**, 30799–30804 (2020).
30. W. Liu *et al.*, RNA-directed DNA methylation involves co-transcriptional small-RNA-guided slicing of polymerase V transcripts in *Arabidopsis*. *Nat. Plants* **4**, 181–188 (2018).
31. Y. Qi *et al.*, Distinct catalytic and non-catalytic roles of ARGONAUTE4 in RNA-directed DNA methylation. *Nature* **443**, 1008–1012 (2006).
32. F. Wang, M. J. Axtell, AGO4 is specifically required for heterochromatic siRNA accumulation at Pol V-dependent loci in *Arabidopsis thaliana*. *Plant J.* **90**, 37–47 (2017).
33. D. Pontier *et al.*, Reinforcement of silencing at transposons and highly repeated sequences requires the concerted action of two distinct RNA polymerases IV in *Arabidopsis*. *Genes Dev.* **19**, 2030–2040 (2005).
34. R. A. Mosher, F. Schwach, D. Studholme, D. C. Baulcombe, PolIVb influences RNA-directed DNA methylation independently of its role in siRNA biogenesis. *Proc. Natl. Acad. Sci. U.S.A.* **105**, 3145–3150 (2008).
35. T. F. Lee *et al.*, RNA polymerase V-dependent small RNAs in *Arabidopsis* originate from small, intergenic loci including most SINE repeats. *Epigenetics* **7**, 781–795 (2012).
36. Q. Gouil, D. C. Baulcombe, DNA methylation signatures of the plant chromomethyltransferases. *PLoS Genet.* **12**, e1006526 (2016).
37. J. W. Grover *et al.*, Maternal components of RNA-directed DNA methylation are required for seed development in *Brassica rapa*. *Plant J.* **94**, 575–582 (2018).
38. L. Wang *et al.*, Global reinforcement of DNA methylation through enhancement of RNA-directed DNA methylation ensures sexual reproduction in rice. *bioRxiv* [Preprint] (2020). <https://doi.org/10.1101/2020.07.02.185371> (Accessed 3 July 2020).
39. E. Debladis *et al.*, Construction and characterization of a knock-down RNA interference line of *OsNRPD1* in rice (*Oryza sativa* ssp *japonica* cv *Nipponbare*). *Philos. Trans. R. Soc. Lond. B Biol. Sci.* **375**, 20190338 (2020).
40. L. Xu *et al.*, Regulation of rice tillering by RNA-directed DNA methylation at miniature inverted-repeat transposable elements. *Mol. Plant* **13**, 851–863 (2020).
41. S. F. Lo *et al.*, A novel class of gibberellin 2-oxidases control semidwarfism, tillering, and root development in rice. *Plant Cell* **20**, 2603–2618 (2008).
42. J. R. Haag *et al.*, Functional diversification of maize RNA polymerase IV and V subtypes via alternative catalytic subunits. *Cell Rep.* **9**, 378–390 (2014).
43. J. T. Trujillo, A. S. Seetharam, M. B. Hufford, M. A. Beilstein, R. A. Mosher, Evidence for a unique DNA-dependent RNA polymerase in cereal crops. *Mol. Biol. Evol.* **35**, 2454–2462 (2018).
44. M. El-Shami *et al.*, Reiterated WG/GW motifs form functionally and evolutionarily conserved ARGONAUTE-binding platforms in RNAi-related components. *Genes Dev.* **21**, 2539–2544 (2007).
45. J. M. Wendte *et al.*, Functional dissection of the Pol V largest subunit CTD in RNA-directed DNA methylation. *Cell Rep.* **19**, 2796–2808 (2017).
46. F. Tan *et al.*, Analysis of chromatin regulators reveals specific features of rice DNA methylation pathways. *Plant Physiol.* **171**, 2041–2054 (2016).
47. F. Tan *et al.*, DDM1 represses noncoding RNA expression and RNA-directed DNA methylation in heterochromatin. *Plant Physiol.* **177**, 1187–1197 (2018).
48. L. Hu *et al.*, Mutation of a major CG methylase in rice causes genome-wide hypomethylation, dysregulated genome expression, and seedling lethality. *Proc. Natl. Acad. Sci. U.S.A.* **111**, 10642–10647 (2014).
49. S. E. Parkinson, S. M. Gross, J. B. Hollick, Maize sex determination and abaxial leaf fates are canalized by a factor that maintains repressed epigenetic states. *Dev. Biol.* **308**, 462–473 (2007).
50. Z. Wang *et al.*, Polymerase IV plays a crucial role in pollen development in *Capsella*. *Plant Cell* **32**, 950–966 (2020).
51. K. F. Erhard Jr *et al.*, RNA polymerase IV functions in paramutation in *Zea mays*. *Science* **323**, 1201–1205 (2009).
52. J. E. Dorweiler *et al.*, *mediator of paramutation1* is required for establishment and maintenance of paramutation at multiple maize loci. *Plant Cell* **12**, 2101–2118 (2000).
53. L. Sidorenko *et al.*, A dominant mutation in *mediator of paramutation2*, one of three second-largest subunits of a plant-specific RNA polymerase, disrupts multiple siRNA silencing processes. *PLoS Genet.* **5**, e1000725 (2009).
54. J. L. Stonaker, J. P. Lim, K. F. Erhard Jr, J. B. Hollick, Diversity of Pol IV function is defined by mutations at the maize *rrm7* locus. *PLoS Genet.* **5**, e1000706 (2009).
55. L. Wei *et al.*, Dicer-like 3 produces transposable element-associated 24-nt siRNAs that control agricultural traits in rice. *Proc. Natl. Acad. Sci. U.S.A.* **111**, 3877–3882 (2014).
56. S. Moritoh *et al.*, Targeted disruption of an orthologue of *DOMAINS REARRANGED METHYLASE 2*, *OsDRM2*, impairs the growth of rice plants by abnormal DNA methylation. *Plant J.* **71**, 85–98 (2012).
57. R. C. Kirkbride *et al.*, Maternal small RNAs mediate spatial-temporal regulation of gene expression, imprinting, and seed development in *Arabidopsis*. *Proc. Natl. Acad. Sci. U.S.A.* **116**, 2761–2766 (2019).
58. D. Cuerda-Gil, R. K. Slotkin, Non-canonical RNA-directed DNA methylation. *Nat. Plants* **2**, 16163 (2016).
59. A. Zemach *et al.*, The *Arabidopsis* nucleosome remodeler DDM1 allows DNA methyltransferases to access H1-containing heterochromatin. *Cell* **153**, 193–205 (2013).